

III-1

Accelerators and
Instruments

BL3U

Soft X-ray Absorption Spectroscopy in the Low Energy Region Explored by the Argon Gas Window

M. Nagasaka^{1,2}¹Institute for Molecular Science, Okazaki 444-8585, Japan²The Graduate University for Advanced Studies, SOKENDAI, Okazaki 444-8585, Japan

Soft X-ray absorption spectroscopy (XAS) is an element specific method to investigate local electronic structures of materials. Since soft X-rays are strongly absorbed by air and liquids [1], XAS spectra of gas and solid samples under an ultrahigh vacuum condition have been extensively studied. Recently, several groups measured XAS spectra in an atmospheric condition by using the high soft X-ray transmission of helium gas. A differential pumping system is used between a soft X-ray beamline under an ultrahigh vacuum condition and a measurement chamber in an atmospheric helium condition [2]. However, the helium gas window is not able to apply XAS in the low energy region below 200 eV since transmitted soft X-rays mostly consist of high order X-rays due to the low transmission of first order X-rays. In this study, we propose the argon gas window for the newly soft X-ray transmission window in the low energy region covering K-edges of Li and B and L-edges of Si, P, S, and Cl [3].

The experiments were performed at soft X-ray beamline BL3U. The measurement chamber in the atmospheric helium or argon condition is separated by a Si_3N_4 membrane with the thickness of 100 nm from the soft X-ray beamline under an ultrahigh vacuum condition. Soft X-rays under vacuum pass through the Si_3N_4 membrane window, the atmospheric helium or argon environment, and finally reach a photodiode detector. The distance between the Si_3N_4 membrane and the photodiode detector is estimated to be 41 mm.

Figure 1 shows the soft X-ray transmission spectra of argon gas in the low energy region. Argon gas has a role to remove high order X-rays above 240 eV due to the absorption of the Ar L-edge. The absorption peak of the Si_3N_4 membrane around 104 eV is observed in the Si L-edge. When the small amount of dimethyl sulfoxide (DMSO) gas is mixed with the argon gas, we have successfully observed the absorption peaks of DMSO gas at the S L-edge (170 eV), which clearly observes the spectral difference between DMSO/Ar mixed gas and argon gas. These peaks are not able to be observed in the atmospheric helium condition since the ratio of the high order X-rays is extremely high in the helium environment.

Figure 2 shows the XAS spectrum of helium gas, where the small amount of helium gas is mixed in the atmospheric argon condition. The XAS spectrum is derived using the Lambert-Beer law, $\ln(I_0/I)$, where I_0 and I are the transmission signals of argon gas and Ar/He mixed gas, respectively. The spectrum shows the helium resonance energy E_2 of the $n = 2$ double excitation Rydberg series at 60.147 eV [4]. It means

that soft X-rays at the Li K-edge (60 eV) are transmittable in the atmospheric argon condition. As a result, the argon gas window enables us to measure XAS in the atmospheric condition in the low energy region from 60 to 240 eV.

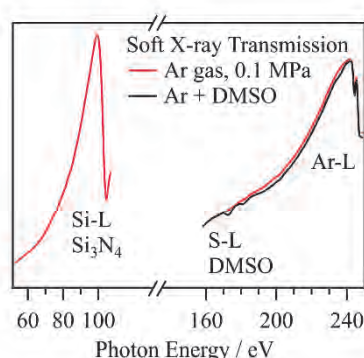


Fig. 1. The soft X-ray transmission spectra of argon gas in the atmospheric condition in the low energy region. The transmission spectrum of argon gas mixed with DMSO gas is also shown.

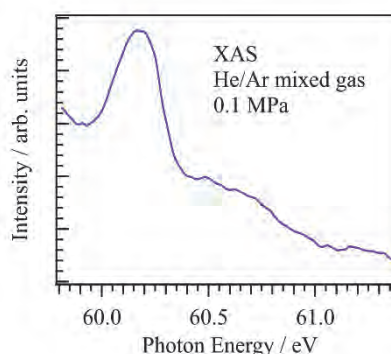


Fig. 2. The XAS spectrum of helium gas mixed with argon gas in the atmospheric condition.

- [1] C. T. Chantler, *J. Phys. Chem. Ref. Data* **29** (2000) 597.
- [2] Y. Tamenori, *J. Synchrotron Rad.* **17** (2010) 243.
- [3] M. Nagasaka, submitted.
- [4] M. Domke *et al.*, *Phys. Rev. A* **53** (1996) 1424.

BL4U

Microscopic Study of Li K-edge

T. Ohigashi^{1,2} and H. Yuzawa¹

¹UVSOR Synchrotron Facility, Institute for Molecular Science, Okazaki 444-8585, Japan

²School of Physical Sciences, The Graduate University for Advanced Studies, SOKENDAI, Okazaki 444-8585, Japan

Lithium is the lightest solid element and is a main element for a lithium ion battery (LIB). Currently, the LIBs are widely used and are essentials in our lives as energy storage devices. Demand of the LIBs is still increasing and higher performance is expected. However, behavior of lithium in the LIB, such as distribution and chemical state during charge/discharge process, is still unclear. To elucidate this process, it is necessary to develop an analytical tool which can analyze lithium with high spatial resolution. So far, analyses of lithium by using an Auger electron microscope [1], a transmission electron microscope with electron energy loss spectroscopy [2] and a secondary ion mass spectroscopy were reported [3]. In addition to these instruments, a scanning transmission X-ray microscope (STXM) also can be a powerful technique. STXM performs X-ray absorption spectroscopy with high spatial resolution in transmission mode. This technique is bulk sensitive and lower damage to a sample [4]. To analyze lithium by STXM, it is necessary to have an access around 55 eV, Li K-edge. This low energy region makes the Li K-edge analyses difficult because tremendous higher order harmonics from a monochromator should be suppressed to obtain X-ray absorption spectra of high quality. Furthermore, focal length of a Fresnel zone plate (FZP) depends on energy of an incoming X-ray so that focal length of the FZP around Li K-edge is typically too short (e.g. 266 μm by the FZP with 25 nm outermost zone width) to construct microbeam optics. Additionally, efficiency of the FZP is low. In this study, we overcame these issues by designing a FZP with a new concept [5].

The optics of STXM at BL4U, a combination of the FZP with chromatic aberration and a pinhole (OSA, order select aperture) is not only to produce a microbeam but also to work as a linear monochromator. This optics theoretically suppresses the higher order harmonics at odd diffractive orders larger than 3rd and cut off even diffractive orders. We designed the new FZP for analysis below 100 eV. The concept of the new FZP is a combination of a phase FZP and a substrate as a low pass filter. Then, the silicon substrate was chosen because of high transmittance of main harmonics, from 50 to 100 eV, and cut-off by Si L₂ and L₃ edge above 100 eV. The parameters of the new FZP are as follows; diameter of 240 μm , outermost zone width of 60 nm, 1,000 zones and gold pattern on silicon substrate of thickness of 200 nm. The focal length of the new FZP is 639 μm at 55 eV. Intensities of the higher order harmonics was evaluated by changing the focal position of the FZP, f , along an optical axis, such as $2f$, $3f$, $4f$, and

$5f$ which are corresponded with focal length of +1st diffractions of 2nd, 3rd, 4th and 5th higher harmonics respectively. Then intensity of the 3rd order harmonics, which is the strongest diffractive order, was suppressed less than 0.1 %.

As a test measurement, Li K-edge of a droplet of LiCl solution on a TEM grid was measured by using a conventional FZP and the new one. Figure 1 (a) show an STXM image of the droplet at 60 eV. In Fig. 1 (b), the spectrum analyzed by the new FZP obviously shows some peaks compared to the conventional one. From comparison with Fig. 1 (b) and spectra in reference [6], the droplet of LiCl reacted with CO₂ in the air and became mixture of LiCl and Li₂CO₃. As an evaluation of spatial resolution, another FZP with the outermost zone width of 36 nm was measured and line and its space pattern of 72 nm pitch was resolved. This resolution implies diffraction limit of the STXM optics with the new FZP.

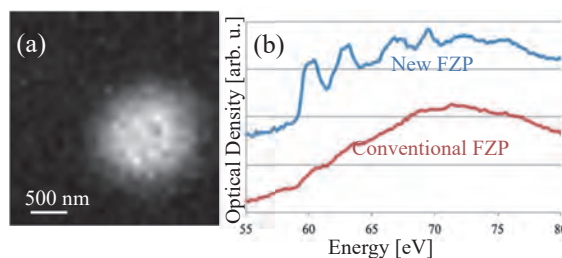


Fig. 1. STXM measurement at Li K-edge of a droplet of LiCl solution, (a) an STXM image at 60 eV and (b) its spectra by using the new and the conventional FZPs.

- [1] N. Ishida, H. Fukumitsu, H. Kimura and D. Fujita, *J. Power Sources* **248** (2014) 1118.
- [2] J. Kikkawa, T. Akita, M. Tabuchi, M. Shikano, K. Tatsumi and M. Kohyama, *Electrochem. Solid-State Lett.* **11** (2008) 399.
- [3] H. Masuda, N. Ishida, Y. Ogata, D. Ito and D. Fujita, *J. Power Sources* **400** (2018) 527.
- [4] R. Qiao, Y-D. Chuang, S. Yan and W. Yang, *PLOS ONE* **7** (2012) e49182.
- [5] T. Ohigashi, in preparation
- [6] J. Tsuji, H. Nakamatsu, T. Mukoyama, K. Kojima, S. Ikeda and K. Taniguchi, *X-Ray Spectrom.* **31** (2002) 319.

Development of Long-term Stable Nuclear Emulsion for Cosmic-ray Imaging

A. Nishio, K. Morishima, K. Kuwabara, T. Yoshida and M. Nakamura
Graduate School of Science, Nagoya University, Nagoya 464-8602, Japan

Cosmic ray imaging is the a new non-destructive inspection technique of large-scale constructions with cosmic ray muon. Cosmic ray muon has high penetrating power and it always comes from the whole sky. In the same way of taking a X-ray photograph, we can obtain integrated density of constructions which thickness are several tens cm to several km. We had ever applied this technique to the pyramid of khufu at Egypt, and discovered a large void [1].

In cosmic-ray imaging observations, we used nuclear emulsion as a detector. Nuclear emulsion is a kind of photographic film and has sensitivity for ionizing radiation. The film record tracks of charged particle with angular accuracy under several mrad. In Nagoya University, started a emulsion gel production machine in 2010. It was enable us to develop new-type emulsion gel by ourselves.

We have succeeded to develop the Long-term Stable Nuclear Emulsion for the purpose of long-term observation of cosmic ray imaging. The problem was Latent image fading which is phenomenon decreasing Grain density (GD, indicator of sensitivity) with time. To enable long-term observation and outdoor use throughout the year, we investigated factors that affect the latent image fading of nuclear emulsion. We found that gelatin, additive chemicals, and packing material affected. The developmental version of newly nuclear emulsion are shown in Table 1.

The latent image fading characteristics of Versions 1 to 5 were investigated. The test was conducted at a temperature of 30 °C and a humidity of 40 % RH. Version 5 was also tested at a humidity of 20 % RH. The results are shown in Fig. 1. Figure 2 shows optical micrographs of tracks on days 0, 30, and 180.

The new stable nuclear emulsion achieved its goal of a GD that remained at 25 or more for half a year at 30 °C. The developed stable nuclear emulsion is being used for cosmic-ray imaging observations in the pyramid of Khufu and is expected to be used for future cosmic-ray imaging observations and other elementary particle research.

Table 1. Developmental version history and the components of each version of the nuclear emulsion. Version 1 is a conventional nuclear emulsion. Versions 2 to 4 are the stages of development, and Version 5 is the stable nuclear emulsion developed.

Version	Gelatin (Volume occupancy of crystals)	Additive chemicals (mol/molAg)			Packing material	
		BTS	Chemical A	Chemical B		Chemical E
1	35 %	1.0×10^{-4}	-	-	-	Melton C
2	35 %	1.0×10^{-4}	-	-	-	Melton C
3	35 %	-	-	-	-	Melton C
4	35 %	-	1.2×10^{-4}	1.2×10^{-4}	1.7×10^{-3}	Melton C
5	35 %	-	1.2×10^{-4}	1.2×10^{-4}	1.7×10^{-2}	ASO

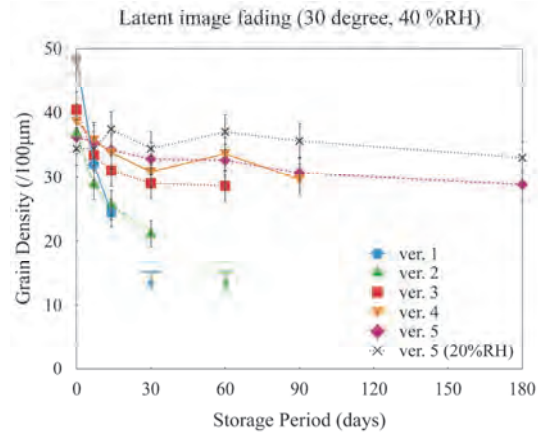


Fig. 1. Latent image fading of Versions 1 to 5 at 30 °C, 40 % RH. The Version 3 samples after day 90 and Version 4 samples on day 180 were impossible to evaluate for the GD due to the large amount of noise.

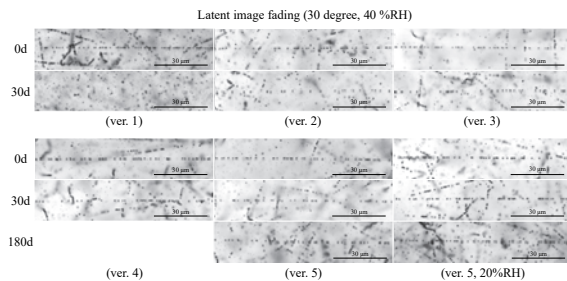


Fig. 2. Optical micrographs of electron beam (several tens of MeV) tracks exposed to Versions 1 to 5 nuclear emulsion on days 0, 30, and 180. Latent image fading at 30 °C, 40 % RH. The length of the black bar is 30 µm. The electron beam was exposed at UVSOR. In the Versions 1, 2, 3, and 4 samples on day 180, there was no track that could be recognized due to the low GD or large amount of noise.

[1] K. Morishima *et al.*, Nature **552** (2017) 386.

BL1U

Construction of Laser Transport System for CHG Experiment at BL1U

M. Hosaka¹, Y. Matsunaga¹, A. Mano¹, Y. Takashima¹, M. Fujimoto² and M. Katoh^{2,3}

¹Nagoya University, Nagoya 464-8603, Japan

²UVSOR Synchrotron Facility, Institute for Molecular Science, Okazaki 444-8585, Japan

³Hiroshima University, Higashi-hiroshima 739-0046, Japan

Coherent harmonic generation (CHG) is a method to imprint external laser information to an electron beam and produce coherent radiation from it with various properties such as polarization [1], temporal and spectral structures [2]. We are planning to conduct the CHG study using an optical klystron and a short pulse Ti:Sa mode lock laser at BL1U. The optical klystron consists of two Apple-II variable polarization undulators and a buncher inserted between them [3]. The laser is injected into the first part of the undulators and energy exchange between it and an electron beam circulating in the storage ring occurs. This leads energy modulation inside the electron beam, that is further converted to density modulation with laser wavelength (micro-bunch) in the buncher section. Coherent radiation is emitted from the micro-bunched beam in the second part of the undulators. Polarization of the emitted radiation can be controlled by tuning the undulator.

In order to perform the CHG experiment, we constructed a laser transport system from the laser room to a laser injection window, whose path length is about 10 m. For simplification, vacuum chamber of the optical klystron is used for laser transportation as seen in Fig.1. The laser is returned to the injection window using a waveplate and a polarization beam splitter. The coherent radiation and the returned laser after the interaction with the electron beam separated using a dichroic mirror. We also prepared a monitoring system to make precise alignment between the laser beam and the electron beam, temporally and spatially.

The CHG experiment was made with an electron energy of 600 MeV. Radiation wavelength of Apple-II undulators was adjusted by changing a magnetic gap length. Fundamental radiation of the first undulator tuned to the wavelength of Ti:Sa laser (800 nm) for the resonant interaction and that of the second undulator is tuned to a wavelength of 267 nm, which corresponds to the 3rd harmonics of the micro-bunching. Spatial alignment between the electron beam and the laser was made looking at radiation from the first undulator. Observed image at the position using a CMOS camera coupled with a telescope is shown in Fig. 2. Laser position in the figure was shifted on purpose and the power was kept low (~10 μ W). The laser beam could be well focused on the electron beam using the monitoring system. We also carried out temporal alignment using a streak camera. Figure 3 shows the measured streak camera images. The laser pulse of 1psec could be well overlapped on the synchrotron radiation (the electron beam) of 100 psec. After the alignment, we increased the laser power to 1W (1 mJ per pulse) to generate the CHG. We used the streak camera and a narrow band pass filter (2 nm-FWHM) for

the observation but no signal arising from the CHG could be seen. We noticed that focusing position of the laser moved considerably with increased laser power. This weakened the laser electric field at the interaction point and suppressed the CHG. We think that the degradation of focusing comes from non-linear effects in transmission type optical elements such as polarization beam splitters. We are planning to remodel the laser transport system for the experiment.

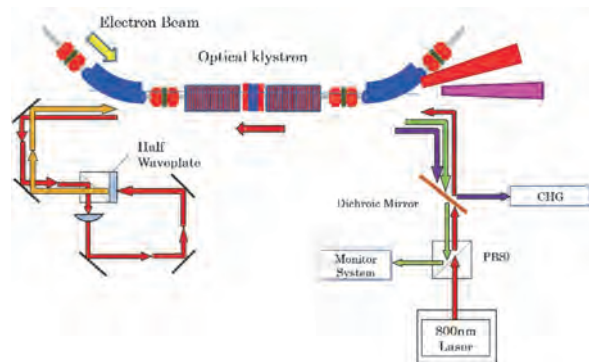


Fig. 1. Schematic of the laser transport system.

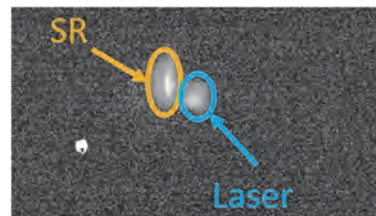


Fig. 2. SR and laser image at interaction point. Electron beam size is around 0.5 mm.

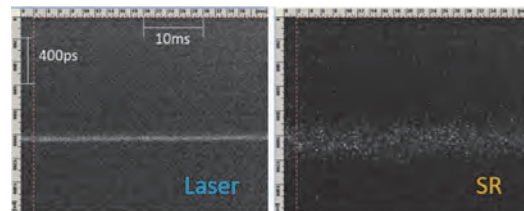


Fig. 3. Streak camera images of SR and laser. The vertical axis is synchronized with accelerator RF signal.

- [1] M. Labat *et al.*, Phys. Rev. Lett. **102** (2009) 014801.
- [2] S. Bielawski *et al.*, Nat. Phys. **4** (2008) 390.
- [3] M. Adachi *et al.*, Proc. IPAC' **10** (2010) 2573.

BL1U

Feasibility Study of Measurement of Polarized Pulsed Gamma-ray by Laser Compton Scattering at 90°

Y. Takashima¹, M. Hosaka¹, U. Shikano¹, A. Mano¹, M. Fujimoto² and M. Katoh^{2,3}

¹*Synchrotron Radiation Research Center, Nagoya University, Nagoya 464-8603, Japan*

²*UVSOR Synchrotron Facility, Institute for Molecular Science, Okazaki 444-8585, Japan*

³*HiSOR, Hiroshima University, Higashi-hiroshima, 739-0046, Japan*

Ultra-short pulse gamma-rays of the pulse width of several picoseconds are generated in UVSOR by 90° scattering of short pulse laser with the electron beam circulating in the storage ring [1]. When the laser is circularly polarized, it is expected that gamma rays generated by Compton scattering are also circularly polarized. There have been some experiments conducted to confirm the polarization of gamma rays generated by the head-on collision of the electron beam and the laser [2]. However, there are no experiments performed to measure the polarization of gamma rays generated in the condition of which the laser and the electron beam collided at a 90° in a laboratory system.

We performed measurements of the spatial distribution of gamma-rays by laser Compton scattering at 90° as a feasibility study to measure the polarization of gamma-rays. In the experiment, we stored 750 MeV electron beam of 30 mA as a single bunch. We used a mode-locked Ti:Sa laser synchronized to the RF frequency of the storage ring. The wavelength and the pulse power of the laser were 800 nm and 1.5 mJ/pulse, respectively. In order to change the direction of the polarization of the laser, we installed a $\lambda/2$ waveplate in front of the injection window on the beam duct of the storage ring. The maximum energy of the gamma-ray is about 6.6 MeV. Figure 1 shows the spectrum of the scattered gamma-rays detected by a NaI scintillator.

We installed photostimulable phosphor plates after the extraction window of BL1U in order to measure the spatial distribution of the gamma-rays. The size of the plate was 11.5 cm x 11.5 cm, and the resolution is 100 μm . Figure 2 show the images of spatial distributions of the gamma-rays generated by 90° scattering of the laser and the electron beam. Fig. 2(a) is the image obtained by the Compton scattering of the laser with linear polarization perpendicular to the direction of the electron beam in the horizontal plane. Fig. 2(b) shows the image by using the laser with linear polarization parallel to the direction of the electron beam. There are some differences in those spatial distributions. The figures indicate that the spatial distribution varies according to the polarization of the incident laser, as suggested by theoretical consideration.

In farther studies, we plan to measure the polarization of the scattered gamma-rays quantitatively by the method of magnetic Compton scattering [2].

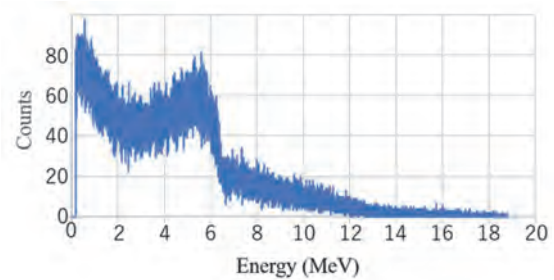


Fig. 1. Energy spectrum of gamma-ray detected by NaI scintillator.

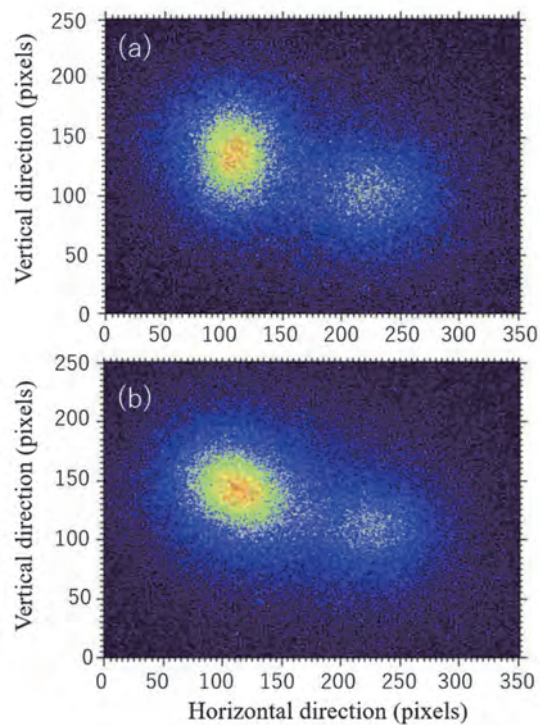


Fig. 2. Spatial distribution of gamma-rays detected by photostimulable phosphor plates. (a) is the image using the horizontally linear polarized laser, and (b) is the image using the laser with linear polarization parallel to the direction of the electron beam.

[1] Y. Taira *et al.*, Nucl. Instrum. and Meth. A **637** (2011) S116.

[2] M. Fukuda *et al.*, Phys. Rev. Lett. **91** (2003) 164801.

BL1U

Study on Isotope 3D Imaging Using NRF Absorption Method in UVSOR-BL1U

H. Ohgaki¹, H. Zen¹, T. Kii¹, K. Ali¹, T. Hayakawa², T. Shizuma², H. Toyokawa³, Y. Taira³, V. Iancu⁴, V. G. Turturica⁴, M. Fujimoto⁵ and M. Katoh⁵

¹Institute of Advanced Energy, Kyoto University, Kyoto 611-0011, Japan

²Tokai Quantum Beam Science Center, National Institutes for Quantum and Radiological Science and Technology, Tokai 319-1106, Japan

³National Institute of Advanced Industrial Science and Technology (AIST) Tsukuba Central 2-4, Tsukuba 305-8568, Japan

⁴Extreme Light Infrastructure - Nuclear Physics, s/ Horia Hulubei National Institute for R&D in Physics and Nuclear Engineering, Bucharest-Magurele, Judet Ilfov, RO-077125, Romania

⁵UVSOR Synchrotron Facility, Institute for Molecular Science, Okazaki 444-8585, Japan

A Nuclear Resonance Fluorescence (NRF) method is a powerful tool for investigation not only of the nuclear physics but also of isotope imaging inside the spent nuclear fuel canisters and nuclear wastes. We have been developing an isotope imaging technique by using NRF [1] as well as by Nuclear Resonance Absorption (NRA) [2].

A demonstration experiment of the NRF-CT imaging by using a LCS gamma-ray beam with a natural lead target has been carried out at the LCS gamma-ray beamline BL1U at UVSOR-III [3]. In 2019, two enriched isotope targets ²⁰⁶Pb (>93.3 %) and ²⁰⁸Pb (>97.8 %) were prepared as the CT target which is made of an aluminum holder as shown in Fig.1.

The LCS gamma-ray beam with a maximum energy of 5.528 MeV was generated by using a fiber laser (wavelength of 1,896 nm, 50 W). The gamma-ray beam with a flux of approximately 1×10^8 photons/s was used for the experiment with a 1-mm lead collimator and the excited $J^\pi = 1^-$ state at 5.512 MeV of ²⁰⁸Pb was populated through NRA. By using the NRF absorption method a NRF-CT image has been taken by 2-mm step in the horizontal direction ($x = -14$ to 14 mm) and 30-deg. step in the rotation angle ($\theta = 0$ to 150°). The NRF signals from the witness target (²⁰⁸Pb enriched) were measured by two Ge detectors with 120 % and 130 % relative efficiencies. At the same time, the transmission gamma-rays have been measured by a $3.5'' \times 4''$ LaBr₃(Ce) detector, which gives a density distribution of the sample target. We have developed the segmented CT reconstruction method [3] and we obtained clear a ²⁰⁸Pb distribution as shown in Fig. 2. On the other hand, by using the γ -ray transmission CT, we cannot distinguish between ²⁰⁶Pb and ²⁰⁸Pb as shown in Fig. 3. We demonstrated the isotope selectivity of the NRF-CT technique at the UVSOR-BL1U beamline.

[1] N. Kikuzawa *et al.*, Appl. Phys. Express **2** (2009) 036502.

[2] H. Zen *et al.*, Energy Procedia **89** (2016) 335.

[3] H. Zen *et al.*, AIP Advanced **9** (2019) 35101.

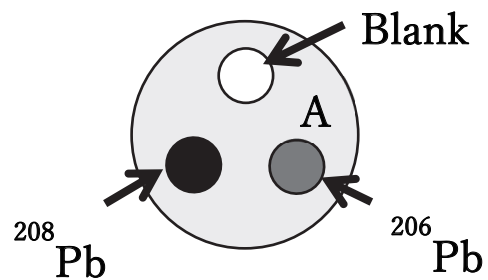


Fig. 1. NRF-CT target.

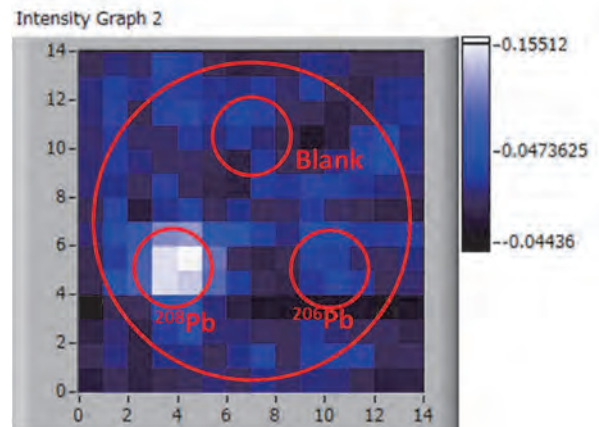


Fig. 2. NRF-CT image.

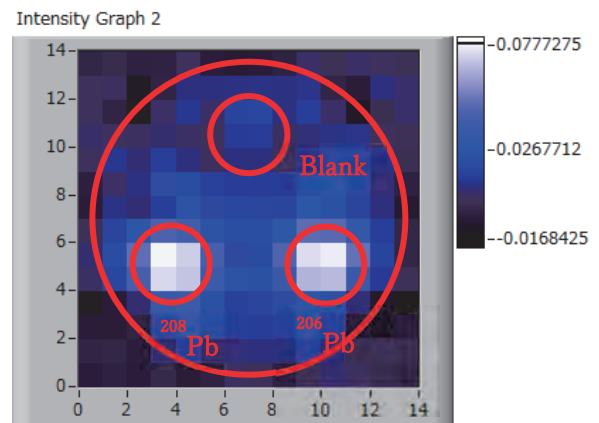


Fig. 3. γ -ray transmission CT image.

BL1U

Study on Temporal Structure of Synchrotron Radiation by Using Interferometer

S. Notsu¹, S. Matsuba², K. Kawase³ and M. Katoh^{1,4}

¹Hiroshima University, Higashi-Hiroshima, 739-0046, Japan

²JASRI, Sayo-cho 679-5198 Japan

³QST, Tokai-mura 319-1106, Japan

⁴UVSOR Synchrotron Facility, Institute for Molecular Science, Okazaki 444-8585, Japan

Temporal structure of synchrotron radiation may be separated into two categories. The first one is the that of a photon wave packet emitted from a single electron. Another temporal structure is the width of the light pulse emitted from a bunch of electrons, which comprises of many wave packets randomly distributing over the length of the electron bunch.

Usually the pulse length of synchrotron radiation, which is typically 10 to 100 psec, is measured with a streak camera. However, there is no report on the direct measurement of the wave packet length. In the laser field, it was demonstrated to measure both the light pulse width and the wave packet length (coherence length) by using an interferometer based on the photon correlation [1]. By using same method, it was demonstrated to measure the pulse width of the bending radiation [2].

We constructed an interferometer as shown in Figs. 1 and 2, which is a modification of Michelson-type interferometer. Two experiments can be conducted on this interferometer. The first one is two-photon correlation and another is autocorrelation. We conducted these experiments by using an undulator beamline BL1U (Fig. 3). We extracted the undulator radiation at a wavelength of 355 nm and introduced it to the interferometer.

The details of the results will be presented in a future paper. Here, we only give a short summary. Concerning two-photon correlation, so far, we could not get a significant result, which gives the information on the pulse length. The reason is presumably on the alignment of two light beams at the detector. We shall improve the alignment method and try this experiment in near future. On the other hand, in the autocorrelation experiment, we can get a promising result on the coherence length. Also, we note that the mechanical vibration produces a significant effect on the results. We shall improve the mechanical stability of the interferometer and try the next experiment in the nearest future.

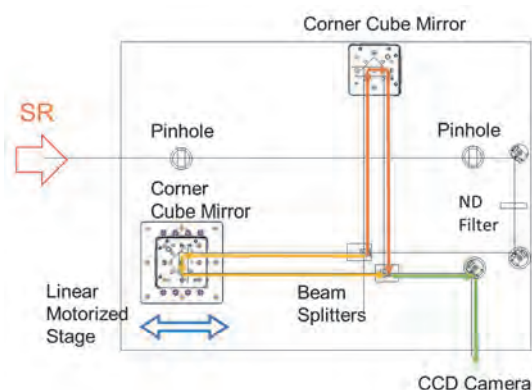


Fig. 1. Interferometer (Autocorrelation setup is shown).

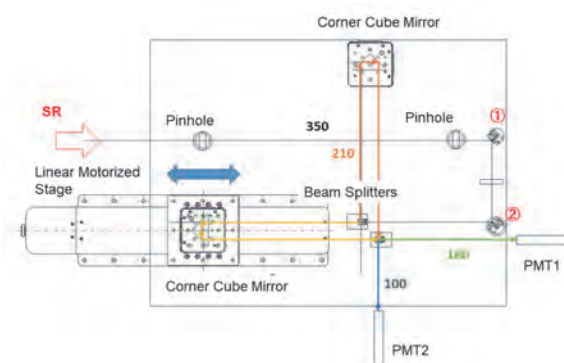


Fig. 2. Interferometer (Two photon correlation setup is shown).

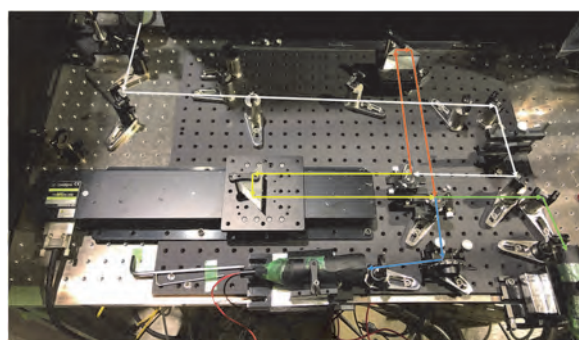


Fig. 3. Interferometer set at BL1U.

[1] Y. Miyamoto *et al.*, Opt. Lett. **18** (1993) 900.

[2] T. Mitsuhashi and M. Tadano, Proc. EPAC2002 (Paris, 2002), 1936.

BL2A

X-ray Transmission Measurements for Optical Blocking Filters on Board the Third Focusing Optics X-ray Solar Imager (FOXSI-3) Sounding Rocket

I. Mitsuishi¹, S. Shimizu¹, T. Yamaguchi¹ and N. Narukage²

¹Nagoya University, Nagoya 464-8601, Japan

²National Astronomical Observatory of Japan, Mitaka 181-8588, Japan

The solar corona is full of dynamic phenomena. They are accompanied by interesting physical processes, namely, magnetic reconnection, particle acceleration, shocks, waves, flows, evaporation, heating, cooling, and so on. The understandings of these phenomena and processes have been progressing step-by-step with the evolution of the observation technology in EUV and X-rays from the space. But, there are fundamental questions remain unanswered, or haven't even addressed so far. Our scientific objective is to understand underlying physics of dynamic phenomena in the solar corona, covering some of the long-standing questions in solar physics such as particle acceleration in flares and coronal heating, and so on. In order to achieve these science objectives, we identify the imaging spectroscopy (the observations with spatial, temporal and energy resolutions) in the soft X-ray range (from ~0.5 keV to ~10 keV) is a powerful approach for the detection and analysis of energetic events [1]. This energy range contains many lines emitted from below 1 MK to beyond 10 MK plasmas plus continuum component that reflects the electron temperature.

For the first imaging spectroscopic observation of the solar corona in soft X-ray range, we launched a NASA's sounding rocket (FOXSI-3) on September 7th, 2018 [2] and successfully obtained the unprecedented data [3] using a combination of X-ray mirror and high speed X-ray camera with a back-illuminated CMOS sensor [4-6].

In this instrument, filters made of thin polyimide films with aluminum coating were deployed to reject the intense visible light from the sun and to adjust the incident X-ray flux into the camera. These optical blocking filters (hereafter OBFs) are located in front of both X-ray optics and the CMOS detector. Actually, we confirmed our OBFs worked successfully during the observation. To achieve our scientific goals, X-ray transmission through OBFs should be taken into account accurately and thus, X-ray transmission measurements were conducted in BL2A as shown in Fig. 1. We took X-ray transmission data at 830, 1000, 1200, 1400, 1600, 1800, and, 2000 eV to obtain a proper model representing the observed transmission. Consequently, the observed thicknesses of polyimide and aluminum coating films are 2.8 μm / 180 nm and 5.0 μm / 320 nm and we extracted the expected models with accuracies of typically <10 % and <5 % for OBFs of X-ray optics and the CMOS detector, respectively as shown in Fig. 2.

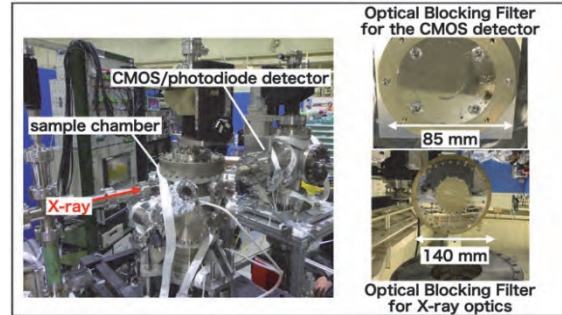


Fig. 1. Overview of our experimental setup (left) and OBFs for X-ray optics (top right) and the CMOS detector (bottom right) on board FOXSI-3.

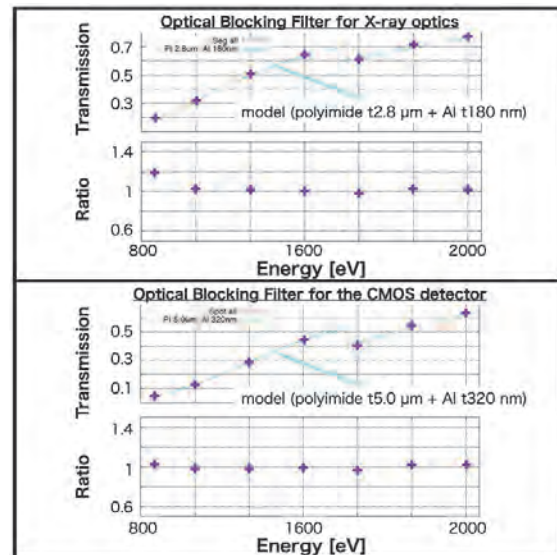


Fig. 2. Observed transmission of OBFs for X-ray optics (top) and CMOS detector (bottom) and the ratio of the observed to the expected value.

- [1] N. Narukage *et al.*, White paper of the “soft X-ray imaging spectroscopy”, arXiv:1706.04536 (2017).
- [2] Web Release: <https://hinode.nao.ac.jp/en/news/topics/foxsi-3-180907/>
- [3] Web Release: <https://hinode.nao.ac.jp/en/news/topics/foxsi-3-data-release-en-20190115/>
- [4] N. Narukage *et al.*, Nuclear Instruments and Methods in Physics Research Section A **950** (2020) 162974.
- [5] S. Ishikawa *et al.*, Nuclear Instruments and Methods in Physics Research Section A **912** (2018) 191.
- [6] N. Narukage and S. Ishikawa, UVSOR Activity Report 2018 **46** (2019) 36.

BL3B

Study on the Electronic State of Fine-grained AgBr:I Crystals by Luminescence under Low Temperatures

T. Naka¹, T. Shiraishi¹, S. Kurosawa² and H. Sone³

¹ Department of Physics, Toho University, Funabashi 274-8510, Japan

² New Industry Creation Hatchery Center (NICHe), Tohoku University, Sendai 980-8577, Japan

³ Industrial Technology Institute, Miyagi Prefectural Government, Sendai 981-3206, Japan

This is a study on the electronic state of AgBr:I nano-crystals in the nuclear emulsion by their luminescence response. The nuclear emulsion in which AgBr:I crystals are dispersed in gelatin is a particle tracking detector with sub-micrometric accuracy. Each crystal behaves a charged particle sensor of the indirect-transition semiconductor. Among electrons and holes excited in the crystal by the ionizing loss of charged particles, a few electrons are contributed to the track (latent image) formation. On the other hand, we found in previous studies that luminescence occurs with high efficiency at below the liquid nitrogen temperature by recombination of electrons and holes through iodine center [1].

For the AgBr:I crystal of the nuclear emulsion, the typical crystals are sub-micro sizes; in particular, a Nano Imaging Tracker (NIT) [2,3] in which super fine-grained crystals of approximately 40 nm are dispersed with a high density of 10,000 crystal/ μm^3 was implemented as a track detector with the world's highest spatial resolution. It is used for the directional dark matter search, neutrons or heavy ions detector. However, their response for charged particles is still under studying. Because the behavior of electrons in nanoscale AgBr:I crystals leads to the greater understanding of the latent image formation mechanism, we study their electronic states, such as electron traps or the band structure, through the luminescence response by photoexcitation. In this year, we compared them with the previous knowledge by using a 200 nm crystal size, which is well understood in photographic science.

In thermo-luminescence measurement, after exciting with 240 nm light at 10 K for 10 min, the luminescence spectrum was measured at a constant temperature increase rate up to 300 K. A result at the rate of 4.9 K/min is shown in Fig. 1. The depth of the electron trap calculated from this measurement was estimated to be several tens meV. This is consistent with the trap due to interstitial silver ions [4], however such a very shallow trap is not considered to be contributed to the latent image formation. It is expected the existence of deeper electron traps by measuring up to more high temperature.

In addition, we measured the excitation spectrum dependency of the luminescence intensity (Fig. 2), and showed that this result was consistent with the predicted band structure by the calculation in bulk crystals [5].

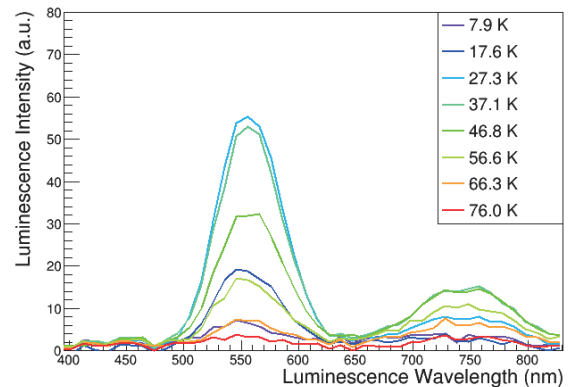


Fig. 1. Thermo-luminescence spectrum of AgBr:I crystal of 200 nm size at temperature increase rate of 4.9 K/min.

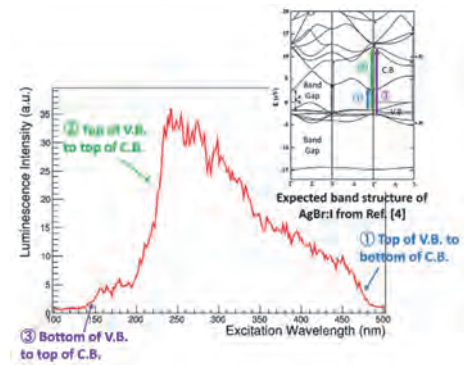


Fig. 2. Excitation spectrum of AgBr:I crystal of 200 nm size at 10 K.

[1] T. Shiraishi, H. Ichiki and T. Naka, Nucl. Inst. Meth. A **927** (2019) 202.

[2] T. Naka *et al.*, Nucl. Inst. Meth. A **718** (2013) 519.

[3] T. Asada, T. Naka, K. Kuwabara and M. Yoshimoto, Prog. Theor. Exp. Phys. **063H01** (2017).

[4] S. Sakuragi and H. Kanzaki, Phys. Rev. Lett. **38** (1977) 1302.

[5] V. Oleshko, M. Amkreutz and H. Overhof, Phys. Rev. B **67** (2003) 115409.

BL4B

Photoelectron Based Soft X-ray Detector for Removing High Order X-rays

M. Nagasaka^{1,2} and H. Iwayama^{1,2}¹Institute for Molecular Science, Okazaki 444-8585, Japan²The Graduate University for Advanced Studies, SOKENDAI, Okazaki 444-8585, Japan

Soft X-ray absorption spectroscopy (XAS) in the low energy region below 200 eV is important to investigate chemical and biological phenomena since this energy region includes K-edges of Li and B and L-edges of Si, S, P, and Cl. However, it is difficult to measure XAS in the low energy region because transmitted soft X-rays mainly consist of high order X-rays due to the low transmission of first order X-rays. There are several techniques for removing high order X-rays, such as metal filters, energy analysis by the silicon drift detector [1], controlling the incident angle of a focused mirror in the beamline [2]. However, these methods are not able to apply the selection of the first order X-rays below 200 eV from those of the high order X-rays. In this study, we have developed a photoelectron based soft X-ray (PBSX) detector that removes contributions of high order X-rays for XAS below 200 eV [3].

The experiments were performed at soft X-ray beamline BL4B. Figure 1 shows schematics of our PBSX detector system, which consists of an Au plate, an Einzel lens, and an MCP detector. Transmitted soft X-rays from a sample film are irradiated to the Au plate, and the emitted Au 4f photoelectrons are collected into the MCP detector with the Einzel lens. The Einzel lens have three electrodes (P1, P2, and P3). V_1 is a constant voltage, whereas V_2 is a pulsed gate voltage. The Au 4f photoelectrons excited by both the first order X-rays and the high order X-rays detects with the gate-off voltage, whereas those excited by the high order X-rays only detect with the gate-on voltage. The photon flux of the first order X-rays is obtained by subtracting the intensities of the photoelectrons with the gate-on voltage from those with the gate-off voltage.

Figure 2 shows Si L-edge XAS spectra of the polymer/SiC film, where the thickness of the polymer (MOXTEK ProLINE) and SiC membrane (NTT AT) is 150 and 100 nm, respectively. Both photodiode (IRD AXUV100) and PBSX detectors are settled behind the sample films. XAS spectra in transmission mode are based on the Lambert-Beer law, $\ln(I_0/I)$, where I_0 and I are the transmission signals of blank and sample, respectively.

As observed in the Si L-edge XAS of SiC wafers [4], the XAS spectra show the large peak around 103.63 eV and small peaks around 112.5, 115.5, 120, and 142 eV. The broad peak is also observed around 158 eV. Since the contributions of the high order X-rays around 97 eV are removed by the PBSX detector, the intensity of the first SiC peak (103.63 eV) becomes higher than that obtained by the photodiode detector. In addition, due to removing the contributions from the fifth order X-rays at the O K-edge, the peak width also becomes narrower and is nearly

same as that in the SiC film. The contribution from the second order X-rays at the C K-edge is also removed in the XAS spectra. As a result, we have successfully measured Si L-edge XAS spectra of the polymer/SiC film with avoiding the contribution of the high order X-rays by using the PBSX detector.

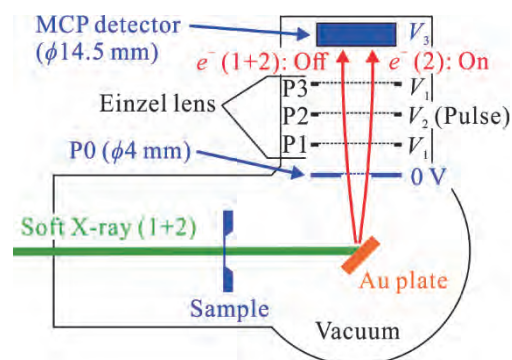


Fig. 1. Schematics of the PBSX detector. Photon flux of the first order X-rays is separately collected from those of the high order X-rays by using the energy difference of the Au 4f photoelectrons.

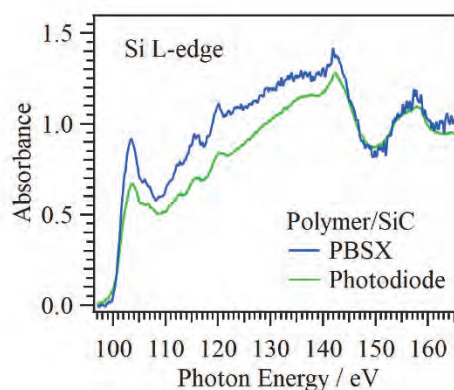


Fig. 2. Si L-edge XAS spectra of the polymer/SiC film by using the photodiode and PBSX detectors.

[1] P. Lechner *et al.*, Nucl. Instrum. Methods Phys. Res. A **377** (1996) 346.

[2] Y. Kitajima *et al.*, J. Electron Spectrosc. Relat. Phenom. **101-103** (1999) 927.

[3] M. Nagasaka and H. Iwayama, in preparation.

[4] S. Muto and T. Tanabe, J. Appl. Phys. **93** (2003) 3765.

BL5B

Multilayer Reflectometry for Evaluation of Second Harmonic Spectral Impurity in 100 nm Wavelength Output of BL5B UVSOR

T. Hatano¹, Y. Matsuda² and T. Ejima¹¹IMRAM, Tohoku University, Sendai 980-8577, Japan²Department of Chemistry, Graduate School of Science, Tohoku University, Sendai 980-8578, Japan

VUV generation of rare gas excited by intense laser pulse can be used for ionization experiments when it is focused using a suitable condenser optics. VUV of a 118 nm wavelength from Xe is used [1], and VUV of a 100 nm wavelength from Ar is proposed as a new source. Al even with an oxide film on the surface is a high reflectance material in VUV region above 160 nm, and LiF overcoat extends the high reflectance region down to 101 nm [2]. Around 100 nm, however, no normal incidence mirror has been developed so far. Therefore, a condenser mirror having a high normal reflectance at 100 nm is demanded for 100 nm wavelength VUV sources. For that purpose, authors are planning to test thick large- k material or Al overcoated with thin small- n material. In any case, characterization accuracy is crucial. The spectral purity of the output of grating monochromators, especially, is important rather than the geometrical alignment in normal incidence reflectance measurements. In the present study, the second harmonic spectral impurity has been investigated at BL5B UVSOR, which is one of most useful beamlines for calibration of optical elements around a wavelength of 100 nm.

A 20 period Al (17 nm)/Si (16 nm) multilayer reflecting 50 nm (24.8 eV) VUV at an angle of incidence of 18.1° was fabricated for the second harmonic detection at 100 nm (12.4 eV). When the monochromator setting is for 100 nm, the multilayer reflection has an additional signal due to the 50 nm second order diffraction of the grating. The detailed analysis of the measured spectral reflectance gives the ratio of the power of the second order light to that of the total output [3]. The measured spectral reflectance at an angle of incidence of 18.1° is shown in Fig. 1 by blue line. The grating and mirror choice of the monochromator was G3M5. The major peak where the grating diffraction order m_G and the multilayer Bragg reflection order m_M are both 1, was found at 24.8 eV. It gives the reflectance at 24.8 eV as 5.4 %.

The second peak was found at 12.4 eV. Orders of the grating diffraction and the multilayer reflection of this peak were assigned as $m_G = 2$ and $m_M = 1$. The evidence can be seen in the spectral reflectance of another multilayer, 15 period Al (50 nm)/Si (17 nm) which is shown in Fig. 1 by green line. This multilayer is similar to the first one if the Si layers were alternatively replaced with Al layer. Therefore it reflects 24.8 eV VUV at a similar angle of incidence of the first one with $m_M = 2$. Two other peaks appeared at lower energy side. There might be a question; which is of the fundamental Bragg reflection ($m_G = 1$ and $m_M = 1$)? The answer is

easy when the dispersion of refractive index n is considered. Since n of Al rapidly decrease from 24.8 eV to 12.4 eV, the $m_M = 1$ peak is expected to appear at much higher energy than 12.4 eV by the refraction effect. Thus, the second peak around 18.6 eV can be attributed to $m_G = 1$ and $m_M = 1$. The third peak located at exactly the half energy of $m_G = 1$ and $m_M = 2$ must be $m_G = 2$ and $m_M = 2$.

Back to the 12.4 eV peak of the first multilayer, the peak height on the baseline of the $m_G = 1$ background reflectance was 2.2 %. It corresponds to the product of the second harmonic ratio and the 24.8 eV reflectance [3]. The conclusion is that 41 % of the monochromator output power is the second harmonic, which means that the experimental result around 100 nm (12.4 eV) must be analyzed with the spectral purity of 59 % at highest taken into account.

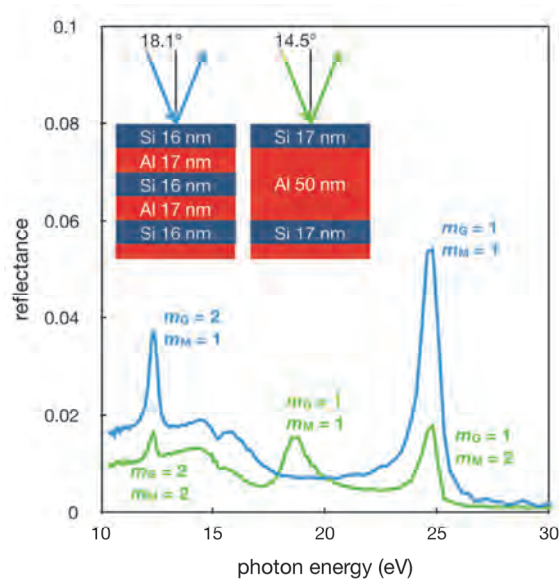


Fig. 1. Measured spectral reflectances of Al/Si multilayers.

- [1] Y. Matsuda, A. Yamada, K. Hanaue, N. Mikami and A. Fujii, *Angew. Chem. Int. Ed.* **49** (2010) 4898.
- [2] W. R. Hunter, J. F. Osantowski and G. Hass, *Appl. Opt.* **10** (1971) 540.
- [3] T. Hatano and T. Harada, *J. Electron Spectrosc. Relat. Phenom.* **196** (2014) 156.

BL5B

Investigation of the Source of the Photon-Energy Drift of BL5B

H. Zen¹, E. Nakamura², K. Hayashi² and K. Tanaka^{2,3}

¹Institute of Advanced Energy, Kyoto University, Uji 611-0011, Japan

²UVSOR Synchrotron Facility, Institute for Molecular Science, Okazaki 444-8585, Japan

³School of Physical Sciences, The Graduate University for Advanced Studies, SOKENDAI, Okazaki 444-8585, Japan

The variation of the photon beam properties, such as beam position, photon energy, and so on, during user operation in the beamline is a big issue in synchrotron radiation (SR) facilities. After introducing the top-up operation in 2010, the average photon flux of the UVSOR has been doubled. Then the heat load on to the mirrors have been doubled and heat induced mirror deformation could induce the variation of the photon beam properties in some beamlines. A photon-energy drift at BL5B has been observed during user experiments [1]. We have started a detailed investigation of the source of the photon-energy drift. Results of our investigation and efforts to reduce the drift are reported.

The first candidate of the source of the photon-energy drift was the M0 mirror, which is water cooled but directly illuminated with SR. At first, a system to monitor the angle of the M0 mirror using a laser diode and a CCD camera was developed to investigate the deformation of M0 mirror and its influence to the photon energy. As the result of the continuous measurement of the photon energy and the M0 mirror angle (Fig. 1), we found that the angle of M0 mirror is not the main source of the photon-energy drift.

The M1 mirror, which is not water cooled, was the second candidate of the source. Several thermocouples were installed to measure the temperature of the M1 mirror and its holder. The measured results of the temperature rise are shown in Fig. 2. After opening the front end valve at 10 o'clock, temperature of M1 mirror and its holder gradually increased. The temperature of the center of the M1 mirror (CH2) was significantly higher than those of the upstream (CH3) and downstream (CH1). This large temperature gradient may cause the deformation of the M1 mirror. Moreover, the temperature of the mirror holder (CH4) has higher temperature than that of M1 mirror. Even after 10 hours from the start of SR injection, the holder temperature continuously increased. This continuous temperature rise could be the source of the continuous photon-energy drift shown in Fig. 1 which lasted for 20 hours.

We found that some stray light of SR directly hit the holder of M1 mirror. This could be the reason why the temperature of the holder (CH4) was higher than that of the M1 mirror (CH2). A horizontal slit after the M0 mirror was adjusted to reduce the amount of the stray light hitting on the M1 mirror holder without significant reduction of SR intensity. This treatment worked well and the amount of temperature rise of the M1 mirror holder could be significantly suppressed from 73 to 57 °C (Fig. 3).

Moreover, a heater was installed to compensate the SR induced temperature rise of M1 mirror. The

temperature of M1 mirror was stabilized by a feedback control. Then the amount of photon-energy drift was decreased from -0.19 to -0.08 eV@73.1 eV. In the present condition, some stray light still hitting on the holder. Further improvement can be achieved by installing a metallic mask in front of the M1 mirror. This will enable us complete cutting out of the stray light and more reduction of the photon-energy drift.

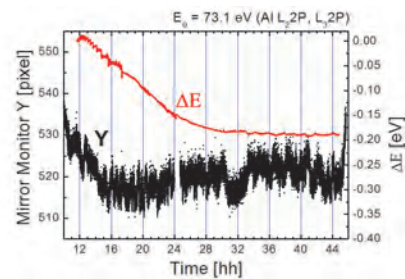


Fig. 1. Result of continuous measurement of the M0 mirror angle and the relative photon-energy of the SR after the monochromator of BL5B.

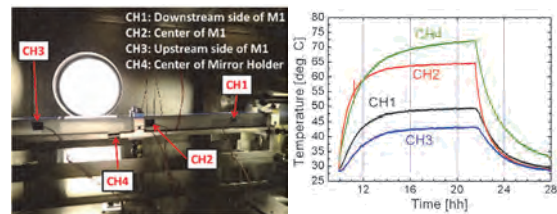


Fig. 2. (Left) Photograph of thermocouples attached to the M1 mirror. (Right) Measured temperature rise.

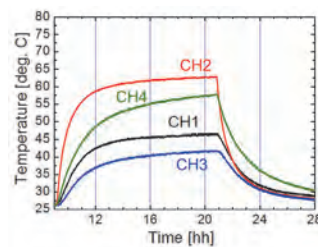


Fig. 3. Measured temperature rise with insertion of slit to reduce the stray light hitting on the holder.

[1] K. Hayashi, UVSOR Activity Report 2011 **39** (2012) 121.

BL7B

Interference Analysis by Composite Type VIS-VUV Complex Refractive Index Measurement Device

J. Omae¹, K. Fukui¹, K. Yamamoto² and T. Saito³

¹Department of Electrical and Electronics Engineering, University of Fukui, Fukui 910-8507, Japan

²Far-infrared region Development Research Center, University of Fukui, Fukui 910-8507, Japan

³Department of Environment and Energy, Tohoku Institute of Technology, Sendai 982-8577, Japan

There is spectroscopic ellipsometry (SE) as a measurement method for obtain accurate complex refractive index spectrum of solid material. However, a commercially available SE device has measurement upper limit of about 5.5 eV. Therefore, based on the instrument designed by the AIST group, we had developed a SE that can measure from visible (VIS) to vacuum ultraviolet (VUV) using BL7B [1].

The VIS-VUV SE can obtain the accurate complex refractive index, but it cannot obtain a wavelength continuous spectrum due to the measurement principle of this SE. On the other hand, there is Kramars-Kronig analysis (KKA) as a method to obtain a wavelength continuous spectrum of complex refractive index. KKA obtains a complex refractive index spectrum through the Kramars-Kronig relation to the reflection spectrum measured in a sufficiently wide wavelength range. However, considering that the quantitative measurement of the reflection spectrum is extremely difficult, the absolute value of the complex refractive index obtained by KKA is uncertain. However, the VIS-VUV SE and KKA have complementary features. Therefore, with the aim of obtaining complex refractive indices spectra from these two analysis methods, we have been incorporating reflectometer into this VIS-VUV SE. However, this combined system cannot take advantage of both features when the measurement target is thin film and the optical interference occurs. Then, in this report, we tried to establish an analytical method in wavelength region where optical interference occurs.

In our combined system, the absolute value of the reflection spectrum obtain by the reflection measurement can be corrected by calculating the reflectance from VIS-VUV SE. The optical interference can be expressed using an appropriate optical model by complex refractive indices n and k . Therefore, applying the fitting calculation with the appropriate optical model to the corrected reflectance spectrum in optical interference energy region allows the complex refractive indices spectra to be obtained directly from the reflection spectrum. Figure 1 shows the corrected reflection spectrum of AlN thin film evaporated on SiO₂ substrate by RF sputtering method. Optical interference was observed at 2 to 5.5 eV, and this analysis was performed in this wavelength region. Figure 2 shows the complex refractive index obtained by this analysis. To evaluate the analysis results, the absorption coefficient was calculated from the

extinction coefficient k , and the shape was compared with the absorption spectrum of this AlN thin film.

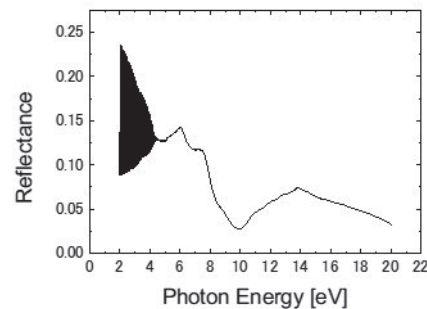


Fig. 1. Reflection spectrum of AlN thin film

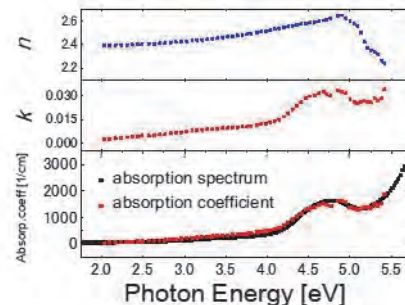


Fig. 2. Complex refractive indices, absorption coefficient and absorption spectrum of AlN thin film

[1] T. Saito, M. Yuri and H. Onuki, Rev. Sci. Instrum. **66** (1995) 1570.

Installation of Momentum Microscope at BL6U

